Applied Clay Science 147 (2017) 11–18

Contents lists available at ScienceDirect

Applied Clay Science

journal homepage: www.elsevier.com/locate/clay

Research paper

Pozzolanic activity of calcined halloysite-rich kaolinitic clays

Alejandra Tironi[a,*], Fernanda Cravero[b], Alberto N. Scian[b], Edgardo F. Irassar[a]

[a] Facultad de Ingeniería, CIFICEN (CONICET-CICPBA-UNCPBA), Av. del Valle 5737, Olavarría, Argentina
[b] Centro de Tecnología de materiales y cerámica, CETMIC (CONICET-CICPBA), Centenario Av. and 506, Gonnet, La Plata, Argentina

ARTICLE INFO

Keywords:
Calcined clay
Halloysite
Kaolinite
Pozzolanic activity
Frattini test
Strength Activity Index

ABSTRACT

The aim of this study is to determine the pozzolanic activity of clays with high content of halloysite/kaolinite, and to evaluate the influence of halloysite/kaolinite ratio and halloysite morphology in the development of pozzolanic activity of the calcined clays. For this purpose, three different natural clays from Río Negro Province, Argentine, were selected and completely characterized. After calcined at 700 °C and ground to 80% of particle size < 45 μm, pozzolanic activity was determined using the electrical conductivity test, the Frattini test and the compressive strength index. Results show that all calcined clays are classified as high reactive pozzolana. The presence of kaolinite and spheroidal halloysite exerts great influence at early ages; while tubular halloysite has greater influence in the pozzolanic activity and the compressive strength of mortars at later ages.

1. Introduction

The use of calcined kaolinitic clays as supplementary cementitious materials (SCMs) has exhibited considerable influence in enhancing the mechanical properties and the durability of mortar and concrete (Siddique and Klaus, 2009). The calcination of a kaolinitic clay at temperature ranging between 500 °C and 800 °C produces the complete dehydroxylation and the formation of an amorphous phase (metakaolin, MK) with high pozzolanic activity (Murat, 1983; Kakali et al., 2001; Siddique and Klaus, 2009; Bich et al., 2009; Tironi et al., 2014a). When kaolinitic clay (1:1) is calcined, the pozzolanic activity is higher than that of calcined 2:1 clays such as montmorillonite and illite (Fernandez et al., 2011; Tironi et al., 2012b; Taylor-Lange et al., 2015; Alujas et al., 2015). Moreover, the compressive strength of blended cements with 30% of calcined kaolinitic clay with medium and high kaolinite content reaches or surpasses the compressive strength of plain Portland cement mortar at 28 days (Tironi et al., 2012a). Additionally, the pozzolanic activity increase when the structural disorder and/or the content of kaolinite increase (Tironi et al., 2014a). Morsy et al. (2010) calcined kaolin nanoclay with a specific surface Blaine (SSB) ≈ 48 m^2/g during 2 h at 750 °C to obtain an active amorphous phase (nano-MK), that was substituted in Portland cement from 0 to 8% by weight. Compressive strength of mortars containing nano-MK increased with the increase of nano-MK content.

Less attention has been paid to the thermal transformation of halloysite than that of kaolinite (Yuan et al., 2015), and the possibility of using it as SCMs. Halloysite and kaolinite have an identical chemical composition, except that halloysite may have as many as two molecules of H_2O, as interlayer water (Churchman et al., 2010). Smith et al. (1993) demonstrated that the thermal transformation of halloysite is largely similar to that of kaolinite. The reaction scheme for the calcination of kaolinite or halloysite initially involves the dehydroxylation between 600 °C and 850 °C, where most of the hydroxyl groups are removed, leading to reduce the coordination of the originally octahedral aluminum (Yuan et al., 2015).

The additional water in the interlayers of halloysite has a decisive influence upon its crystal morphology, which is generally curled rather than platy form as occurred in kaolinite. Common forms are elongated tubes and spheroids (Cravero et al., 2016). For both morphologies different applications have been studied (Yuan et al., 2015; Fernández et al., 2015, Cravero et al., 2016). The nanosized tubular halloysite has an excellent mechanical properties and a very good biocompatibility. These advantages allowed a variety of potential applications in many fields, such as filler in polymers, carrier for the loading and controlled release of guest molecules, adsorbent for pollution remediation, and a nanoreactor/nanotemplate for the synthesis of functional materials (Yuan et al., 2015). The tubular structure of halloysite with one-dimensional mesoporosity or macroporosity allows the encapsulation of various active guests in the lumen of halloysite that acts as nanoscale container, as well as the subsequent controlled release of the guests (Yuan et al., 2015). The use as nanofiller in CPN was effective because halloysite is naturally dispersed, unlike the traditional micron-sized counterparts such as glass fibers and other clay mineral nanofillers such as montmorillonite that have to undergo exfoliation pretreatments to produce nano-layers (Du et al., 2006; Pasbakhsh et al., 2013). The spheroidal halloysite, chemically modified, has given good results for

* Corresponding author.
E-mail address: atironi@fio.unicen.edu.ar (A. Tironi).

http://dx.doi.org/10.1016/j.clay.2017.07.018
Received 27 March 2017; Received in revised form 14 July 2017; Accepted 17 July 2017

petroleum and Ag removal in contaminated waters (Fernández et al., 2015, Cravero et al., 2016).

The incorporation of halloysite in cements was studied by Farzadnia et al. (2013). Tubular hallloysite, with a surface area ≈ 64 m^2/g was substituted in Portland cement with 3% by weight. At 28 days, the compressive strength of mortar increases 24% comparing with the control sample. Considering these results and those obtained when calcined kaolinite was used as SCM, it is expected to get good pozzolanic activity when halloysite is calcined.

Rabehi et al. (2012) studied natural clay composed of halloysite and kaolinite as dominant minerals, and calcite, quartz and illite as impurities. The clay was calcined between 650 and 800 °C and ground to obtain a SSB of 0.56 m^2/g. Calcined clay was used as 0–20% replacement of Portland cement by weight. For 5% replacement, the compressive strength of mortar was 9.88% higher than that of the reference mortar. Tironi et al. (2012a) use calcined kaolinitic clays with SSB from 0.98 to 2.29 m^2/g to elaborate mortars with 30% of replacement. Authors concluded that the SSB of calcined clay has a great importance up to 7 days and then it significance decreased. So a high compressive strength would be expected when the fineness of calcined halloysite clays is increased. It is expected that the increase of the fineness could contribute to improve the pozzolanic activity at the same time as contributing as filler. These studies were carried out using tubular halloysite, but none has been tested on halloysites of spheroidal morphology. In Argentina, halloysite deposits are characterized by the presence of both tubular and spheroidal halloysite, where the latter sometimes predominate. The aim of this study is to determine the pozzolanic activity of Argentinian clays with a high content of halloysite/kaolinite, and to evaluate the influence of the halloysite/kaolinite ratio and the halloysite morphology in the development of the pozzolanic activity of calcined clays.

2. Materials and methods

2.1. Clays

Three different natural clays from Río Negro Province, Argentine, were studied and they are labeled as NC1, NC2, and NC3. NC1-sample comes from Meliqueo deposit and NC2 and NC3-samples are from Pama and Belgrano deposits in the Mamil Choique area (Fig. 1). Halloysite is found in Huitrera Formation (Eocene in age) as an alteration product of volcanic-pyroclastic rocks (Cravero et al., 2016). These clays have high percentage of halloysite and less kaolinite. Spheroidal morphology predominates in almost all the deposits. The chemical composition of natural clays was determined by XRF analysis and it is reported in Table 1. For performing the pozzolanic tests, a Portland cement (PC) was used and its chemical composition is also reported in Table 1. The mineralogical composition of clinker provided by a cement factory was C_3S = 63.6%, C_2S = 15.1%, C_3A = 2.8% and C_4AF = 15%; gypsum (Gyp) is used as set regulator and limestone is the minor component, this phases are identified by XRD (Fig. 2). Its BSS was 0.35 m^2/g.

2.2. Characterization of natural and calcined clays

The mineralogical composition of natural clays was determined by X-ray diffraction (XRD) using a Bruker D2 PHASER diffractometer. Whole rock composition was determined on powder random oriented samples. Oriented films on glass slides were prepared on the < 2 μm fraction obtained by centrifugation of clay-water suspension and were analyzed before and after formamide intercalation, and the halloysite/kaolinite ratio was determined (Churchman et al., 1984; Cravero et al., 2016). FTIR spectrum were obtained using a Nicolet Magna 500 spectrophotometer.

The thermal stability of phases and the temperature range corresponding to the dehydroxylation were analyzed with differential thermal analysis combined with thermal gravimetric analysis (DTA-TG). DTA-TG was carried out using a NETZSCH STA 409 thermobalance. Data obtained by DTA were used to determine the minimum temperature of calcination of these clays to produce the complete dehydroxylation of halloysite and kaolinite (Tironi et al., 2014b). Natural clays morphology was evaluated by Scanning and Transmission Electron Microscopy (SEM, FEI Quanta 200, and TEM, JEOL JSM-100 CX II).

Natural clays (NC) were reduced to particle size < 4 mm and calcined in a programmable laboratory furnace Indef 272 using a fixed bed technique, the heating rate was set at 13 °C per minute. The calcination temperature was selected from the DTA analysis as discussed later. Then, they were ground in a mortar type mill (Fritsch Pulverisette 2) until 80% of mass passed through the 45 μm sieve (#325).

The calcined clays (CC) were analyzed by DTA-TG and XRD to verify that the dehydroxylation was completed, and all halloysite and kaolinite were effectively transformed to amorphous phase MK. XRD was performed using a Philips PW3710 diffractometer. A Rigaku EVO2 Plus device was used to perform DTA-TG analysis, samples were heated at 10 °C/min rate up to 1200 °C under O_2 atmosphere. The CC morphology was evaluated by SEM (FEI Quanta 200). The particle size distribution was determined by Malvern Mastersizer 2000 laser particle size analyzer and the d_{10}, d_{50}, and d_{90} diameters were calculated, and the SSB (Specific Surface Blaine) was determined according to ASTM C 204-04 standard.

Fig. 1. Localization of the halloysite deposits where the studied samples come from NC1: Meliqueo deposit, NC2 and NC3: Mamil Choique area.

Table 1
Chemical analysis of natural clays (C) and Portland cement (PC).

Sample	SiO_2	Al_2O_3	Fe_2O_3	CaO	MgO	SO_3	Na_2O	K_2O	TiO_2	LOI
NC1	47.98	34.85	0.63	0.39	0.13		0.38	0.35	1.72	13.01
NC2	48.08	37.30	0.59	0.16				0.18	1.37	11.77
NC3	54.29	29.86	0.95	0.35	0.47		0.33	0.23	1.34	11.37
PC	20.41	3.86	4.50	63.30	0.70	2.28	0.16	0.85		3.26

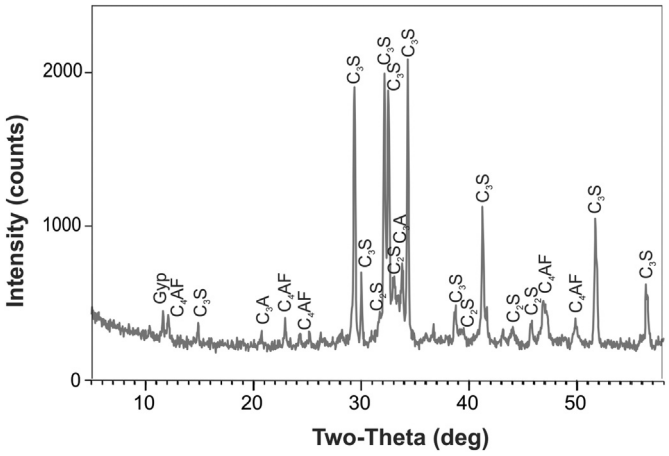

Fig. 2. XRD pattern of Portland cement.

2.3. Pozzolanic activity of calcined clays

The pozzolanic activity of CC was measured by electrical conductivity test, Frattini test and compressive strength (Tironi et al., 2013).

The electrical conductivity (EC) of 20 ml of calcium hydroxide saturated solution of at 40 ± 1 °C, and 2 g of CC was monitored, at regular intervals, using a Jeway 4010 conductivity meter. The EC values decrease with time when CC has pozzolanic activity and reacts with calcium hydroxide, causing a decrease on the ion concentration in the solution (Tironi et al., 2013).

Frattini test was carried out according to the procedure described in EN 196:5 standard. In this method, 20 g of blended cement (25% CC) and 100 ml of boiled distilled water at 40 °C were mixed. At 2, 7, and 28 days the Ca^{2+} and OH^- concentrations in solution were determined. The results are compared with the solubility curve for Ca $(OH)_2$ in an alkaline solution at the same temperature. Calcined clay is considered as active pozzolan when the $[Ca^{2+}]$, $[OH^-]$ in the solution is below the solubility isotherm.

Compressive strength (CS) and flow were assessed on mortars made with standard sand EN-196-1 (1:3), and water to blended cement ratio (w/bc) of 0.50. The replacement of calcined clay by Portland cement used was 25% by weight. The CS was determined as the average of five specimens using universal testing machine Instron 4485 at 2, 7, and 28 days. The Strength Activity Index (SAI) was calculated as the ratio of the CS of blended cement to the CS of the PC-mortar at the same age (Tironi et al., 2012a).

Complementary, the consumption of $Ca(OH)_2$ by pozzolanic reaction was checked by DTA-TG and XRD. For this purpose, pastes were elaborated with blended cements and PC. After 2 and 28 days of hydration fragments of the pastes were immersed in acetone for 24 h and dried overnight in oven at 40 °C. Then, the fragments were ground and passed through a 45 μm sieve (#325) and analyzed by DTA-TG and XRD. The percentage of $Ca(OH)_2$ by mass was determined by DTA-TG between 410 and 560 °C range of dehydroxylation of this phase.

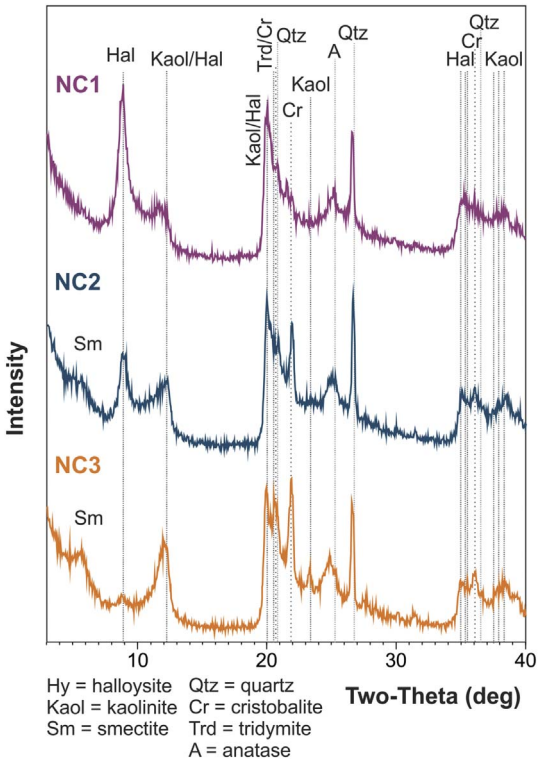

Fig. 3. XRD patterns of natural clays.

3. Results

3.1. Characterization of natural clays

The main clay minerals present in the three samples are halloysite (Hal) and kaolinite (Kaol), with impurities of quartz (Qtz), trydimite (Trd), cristobalite (Cr), and anatase (A), and smectite (Sm) in NC2 and NC3 samples (Fig. 3). The FTIR spectrums of natural clays (Fig. 4) show a OH-stretching band near 3620 cm^{-1} that arises from internal OH groups, and that near 3700 cm^{-1} that arises from internal surface OH groups from kaolinite and halloysite. The weak band near 3570 cm^{-1} present in halloysite may arise from H-bonding between surface OH groups and interlayer water (Russell, 1987).

The halloysite/kaolinite ratio determined was 100/0 Hal/Kaol for NC1, 75/25 Hal/Kaol for NC2 and 60/40 Hal/Kaol for NC3.

The three samples present two endothermic peaks in the temperature range of 20–140 °C and 400–600 °C (Fig. 5) assigned to the loss of physically adsorbed water and the dehydroxylation of halloysite/kaolinite (Cravero et al., 2016), respectively. The dehydroxylation of halloysite, implies the loss of long-range order and the increasing disconnection of the silica and alumina originally in the tetrahedral and octahedral sheets, respectively (Yuan, 2016).

An exothermic peak was also observed in the temperature range of 980–990 °C, and attributed to structural rearrangement of the clay minerals to form mullite (M'barek Jemaï et al., 2015). The largest area of the first endothermic peak and the highest loss of mass in the corresponding temperature range were determined on the NC1 clay, in

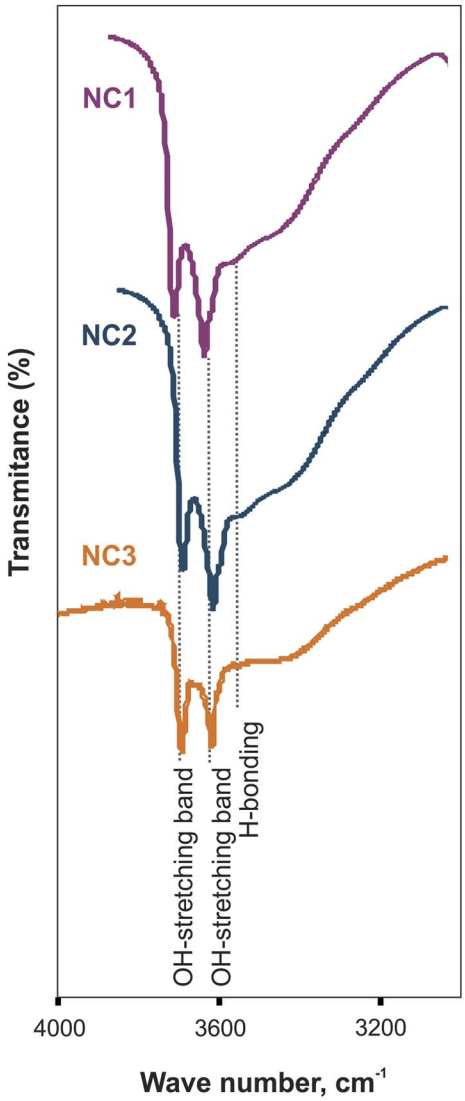

Fig. 4. FTIR spectrums of natural clays.

agreement with the highest content of halloysite as determined by XRD. The mass loss corresponding to the second endothermic peak was used to determine the halloysite/kaolinite content, obtaining 85% for NC1, 80% for NC2, and 75% for NC3. Assuming the complete thermal transformation, the MK content is ~23.8, 21.3 and 20.0 g by 100 g of blended cement for CC1, CC3 and CC3, respectively. On the other hand, the $Ca(OH)_2$ released by complete hydration of Portland cement is ~19.5 g by 100 g of blended cement. As 1 g of MK could combine with a maximum of 1 g of $Ca(OH)_2$ to form cementitious compounds (Tironi et al., 2013), then can be concluded that studied calcined clays have sufficient MK to react with all $Ca(OH)_2$ released by cement hydration.

In order to get the highest amount of amorphous phase (Tironi et al., 2014b), the temperature selected for the heat treatment must be lower than the temperature of formation of the crystalline phase (980 °C), and higher than the temperature corresponding to the end of the last endothermic peak (600 °C). For this reason, the selected temperature for thermal treatment was 700 °C.

The clay minerals present in the natural clays have different morphologies (Fig. 6). The halloysite present in NC1 has a tubular morphology, while the halloysite present in NC2 and NC3 have spheroidal morphology. NC1 has a relatively uniform morphology with good tubule quality and the morphological parameters of nanotubes are 350 nm of length and 117 nm of external diameter (Fig. 6a). NC2 has spheroidal uniform morphology (Fig. 6b), and NC3 has spheroidal halloysite coexisting with hexagonal plates of kaolinite (Fig. 6c).

3.2. Characterization of calcined clays

After thermal treatment at 700 °C, the endothermic peaks assigned to the dehydroxylation of halloysite/kaolinite in DTA-TG disappear (Fig. 7), and the peaks of halloysite and kaolinite also disappear in the XRD-patterns (Fig. 8) indicating the complete dehydroxylation of these phases and their transformation into an amorphous phase (MK). These results agree with the observations reported by Yuan (2016) for halloysite calcined at 600 and 900 °C and the subsequent formation of metahalloysite. Other crystalline phases, such as quartz, cristobalite, trydimite and anatase remain stable.

Thermal treatment did not modify drastically the morphology of the clays (Fig. 9). The tubular morphology is identified in CC1 (Fig. 9a) while the spheroidal morphology is identified in CC2 and CC3 (Fig. 9b and c), and the hexagonal plates are easily identified in CC3 (Fig. 9c). For all samples, tubes and spheres were slightly affected after the dehydroxylation process as reported by Yuan et al. (2012) and Yuan

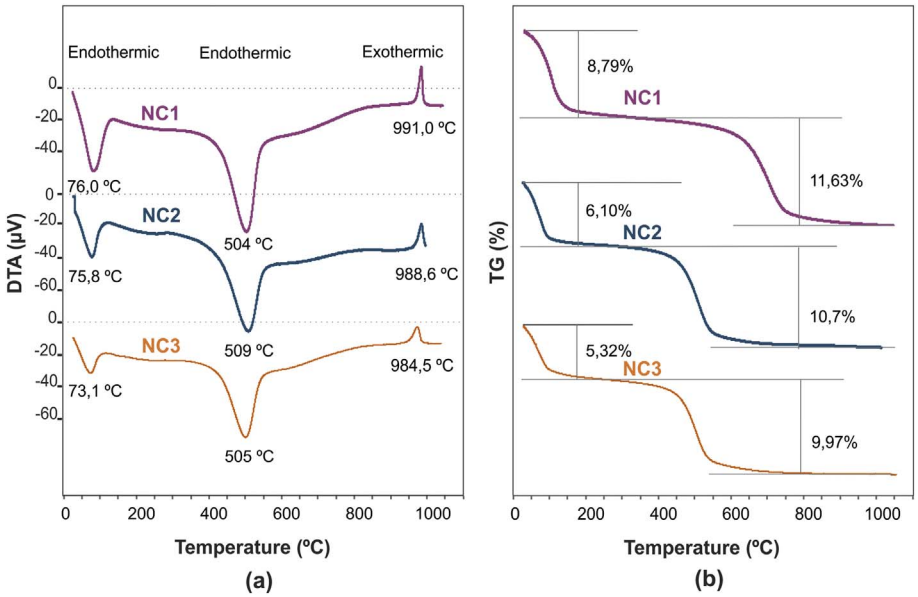

Fig. 5. DTA (a) and TG (b) curves of natural clays.

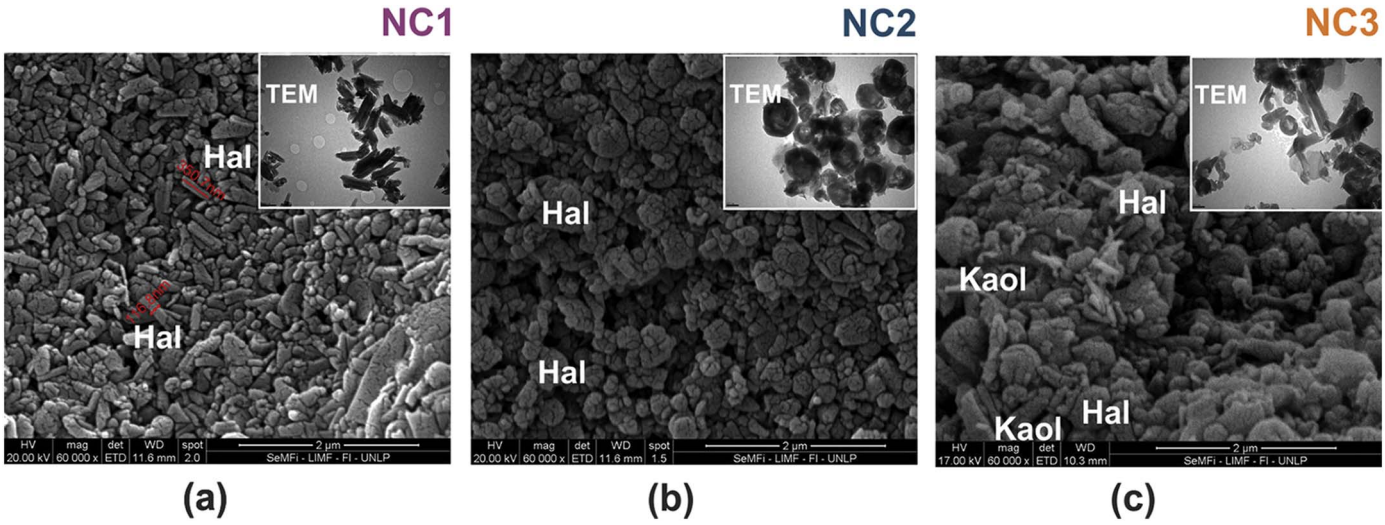

Fig. 6. SEM and TEM micrographs of natural clays NC1 (a), NC2 (b), and NC3 (c).

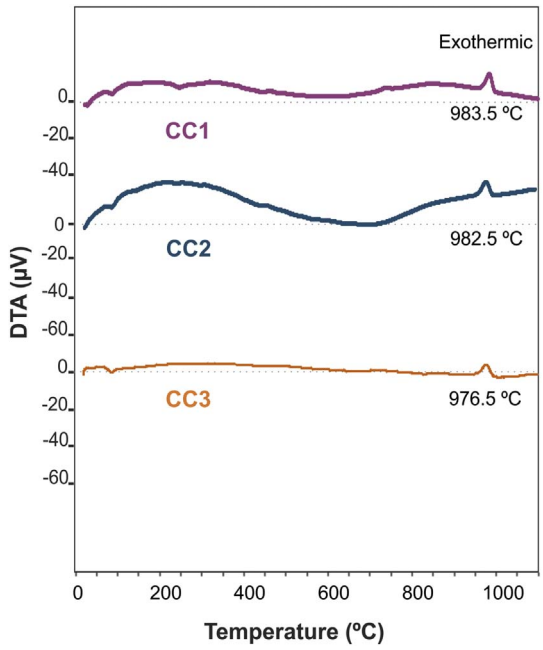

Fig. 7. DTA curves of calcined clays.

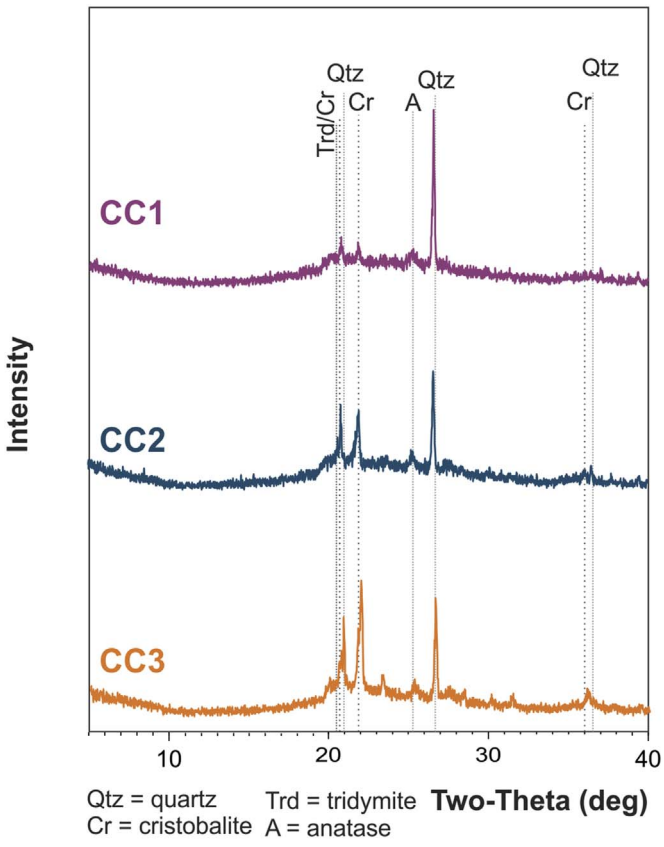

Fig. 8. XRD patterns of calcined clays.

(2016) for calcined tubular halloysite. They investigated the morphological and textural characteristics as well as the surface reactivity and concluded that the tubular structure of halloysite has high thermal persistence. The rough tubular morphology and the mesoporosity of halloysite remained largely intact as long as the heating temperature was lower than 900 °C.

The d_{10}, d_{50}, and d_{90} diameters (Table 2) calculated from the particle size distribution are in the same order of magnitude for all calcined and ground clays. However, CC1 with highest content of tubular halloysite has the highest SSB; and CC2 with spheroidal halloysite and lower kaolinite content than CC3 has the lowest SSB (Table 2).

3.3. Pozzolanic activity of calcined clays

The electrical conductivity (EC) of calcium hydroxide solution after addition of calcined clays recorded as a function of time shows that EC dropped drastically during the first 30 min (Fig. 10), due to the fast reduction of Ca^{2+} and OH^- in the system (Luxan et al., 1989). It is attributed to the fixation of dissolved $Ca(OH)_2$ by calcined clay particles (Yu et al., 1999; Tironi et al., 2013). The EC rate of decreasing in the first 30 min was 12, 5 and 7 for CC1, CC2 and CC3, respectively. These differences are attributed to the variation in the SSB of calcined clays (Table 2), and the different morphology of the calcined clays. For higher SSB and tubular morphology, the drop of EC was higher during the early time. After 24 h, EC was very low and it had a similar value for the three calcined clays, being classified as highly reactive pozzolans.

Results of Frattini test are plot as dots in the $[Ca^{2+}]$ versus $[OH^-]$ graph (Fig. 11). The solubility curve of $Ca(OH)_2$ in alkaline solution demarcates the pozzolanic area below this curve and the non-pozzolanic area above it. During hydration, PC releases $Ca(OH)_2$ causing that the result points are above the solubility curve at all test ages. After

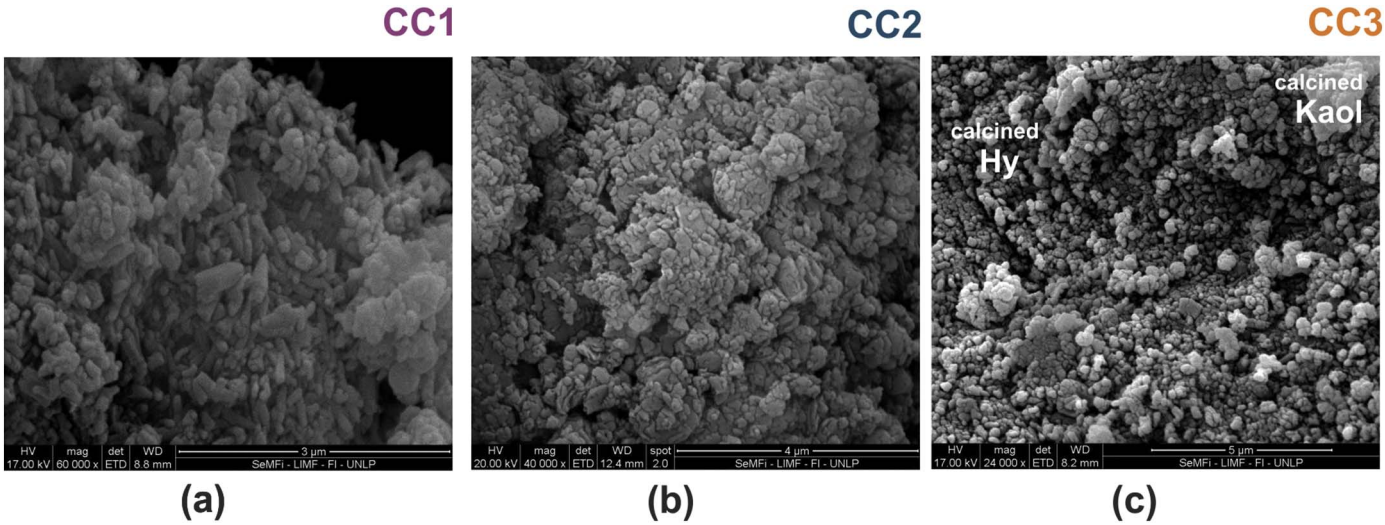

Fig. 9. SEM micrographs of calcined clays CC1 (a), CC2 (b), and CC3 (c).

Table 2
Physical characteristics of calcined clays (CC).

Calcined clay	Particle size distribution, μm			Specific Surface area (Blaine), m^2/g
	d_{10}	d_{50}	d_{90}	
CC1	1.93	7.82	39.54	1.32
CC2	1.50	7.92	22.81	0.95
CC3	1.70	7.50	49.23	1.13

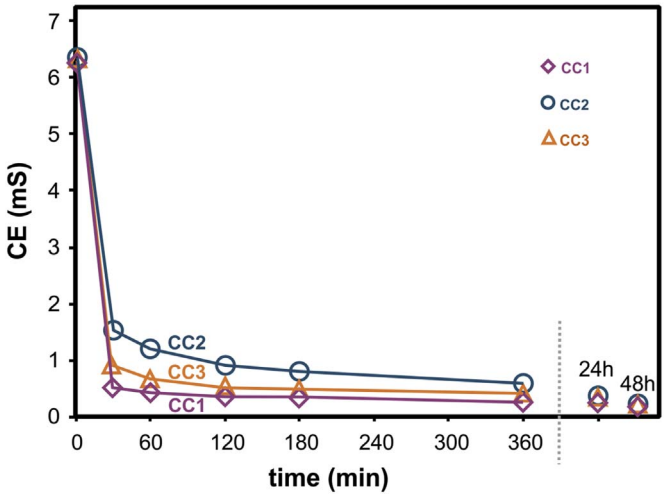

Fig. 10. Electrical conductivity test of calcined clays.

2 days, results of blended cements containing 25% of CC1, CC2 and CC3 are located below the solubility line, indicating that calcined clays have consumed some part of $Ca(OH)_2$ released by PC due to pozzolanic reaction. At this time, the [CaO] and [OH^-] reduction was greater for CC3 (the vertical distance between the point and the solubility curve is larger), at day 7 for CC2, and at day 28 for CC1. Results indicate that blended cement containing CC present high pozzolanic activity after 2 days when the content of halloysite respect to kaolinite is 60/40, and the halloysite has spheroidal morphology; after 7 days when content of spheroidal halloysite is higher; and after 28 days when the clays contain only halloysite as clay mineral and has tubular morphology. Summarizing, the pozzolanic activity is very good for all calcined halloysite/kaolinitic clays, and considering that the thermal treatment does not modify drastically the morphology characteristics of the clays, this

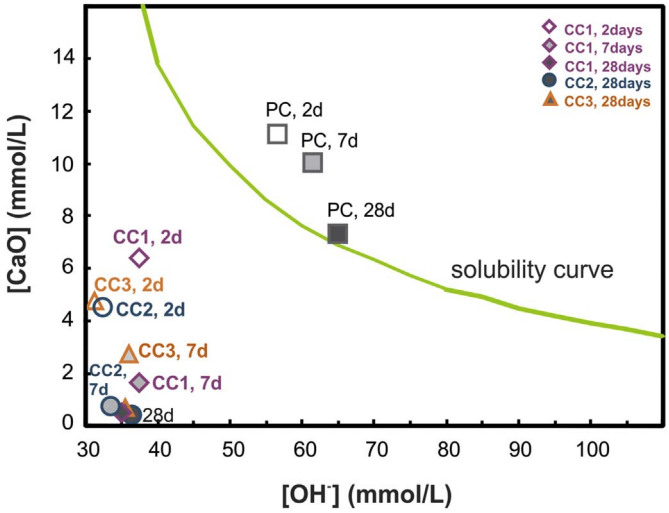

Fig. 11. Results of Frattini test at 2, 7, and 28 days.

characteristic influences in the reactivity, resulting a pozzolana more efficient at early age when the morphology is spheroidal; and a pozzolana more efficient at long age when the morphology is tubular. The highest SSB of CC1 with tubular morphology is not sufficient to asegurate the highest pozzolanic activity at 2 days.

The flow of mortars elaborated with blended cements was determinate and compared with the flow of PC-mortar. For PC-mortar, the flow was 125%, while very low values were determined for blended cements-mortars: 20% for CC1, 14% for CC2 and 54% for CC3. The decrease in flow is a non-favorable effect that should be improved by using superplasticizers. This effect was lower when CC3 is used, obtained from clay with low content of halloysite.

Compressive strength (CS) of mortars elaborated with blended cements and PC are shown in Fig. 12, and the SAI (Strength Activity Index) calculated is summarized in Table 3.

At 2 days, it can be observed that the addition of 25% of CC in blended cements causes a reduction in the CS respect to PC-mortar, indicating that the contribution of pozzolanic reaction cannot compensate the reduction of early reactive Portland cement (dilution effect). However, when SAI is calculated, the value obtained for blended cements with kaolinite and spheroideal halloysite (CC2 and CC3 Table 3) is higher than 0.75, value corresponding to dilution effect (Tironi et al., 2013); whereas for CC1 with tubular halloysite the value obtained (0.74) is mainly attributable to the dilution effect. For blended

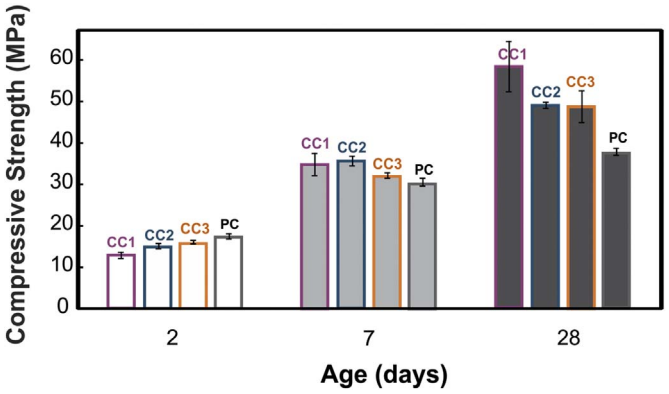

Fig. 12. Compressive strength of mortars at 2, 7, and 28 days.

Table 3
Strength Activity Index (SAI) for mortars elaborated with blended cements containing 25% replacement.

Mortar	Strength Activity Index		
	2 days	7 days	28 days
CC1	0.74	1.14	1.54
CC2	0.87	1.17	1.30
CC3	0.91	1.06	1.29

cements, the higher value of CS was developed by the mortar CC3, followed by CC2 and finally CC1. These results are in agreement with the Frattini test results (Fig. 8), therefore, it can be concluded that, in addition to the filler effect, the pozzolanic effect contributes to CS at early age, being greater when greater is the reactivity of the CC, but not sufficient to overcome the dilution effect.

At 7 days, the CS for all mortars elaborated with blended cements exceeded the mortar-PC. The highest CS was obtained for CC2 (SAI 1.17), followed for CC1 (SAI 1.14), and finally CC3 (SAI 1.06). At 28 days, the compressive strength of blended cement increased significantly compared with the PC and it was 54% higher for CC1 blended cement (SAI 1.54). The calcined clay CC1 obtained from clay with tubular halloysite was classified with the highest pozzolanic activity at 28 days according to the Frattini test, and developed the highest compressive strength at this age.

Finally, the $Ca(OH)_2$ consumption by pozzolanic reaction was confirmed by DTA-TG and XRD in hydrated pastes (Fig. 13). At 2 days, the lower intensity of the peak assigned to this phase (Two-Theta = 18,08°) was registered for CC3 (2.33% $Ca(OH)_2$ in mass determined by DTA-TG, 6.80% for CC1, and 12.75% for PC) confirming the early pozzolanic reaction of this calcined clay; whereas at 28 days a decrease in intensity of the peak of $Ca(OH)_2$ occurred for all calcined clays and the greater reduction was obtained for CC1 (5.68% $Ca(OH)_2$ in mass determined by DTA-TG, 6.38% for CC3, and 16.93% for PC).

4. Discussion

The adequate thermal treatment of clays with halloysite and kaolinite as dominant minerals produces pozzolanic materials (Figs. 10 and 11), but the milling is an important factor too. Rabehi et al. (2012) studied calcined clays of these type with SSB of 0.56 m^2/g, and at 28 days a compressive strength of mortar 9.88% higher than the reference mortar was obtained; whereas in this study the SSB was between 0.95 and 1.30 m^2/g (Table 2), and at 28 days the compressive strength of mortar was 29–54% higher than the reference mortar (Fig. 12). When halloysite with tubular structure and surface area of 64 m^2/g was used by Farzadnia et al. (2013), the compressive strength increased 24% for 3% nanoclay at 28 days, results comparables with

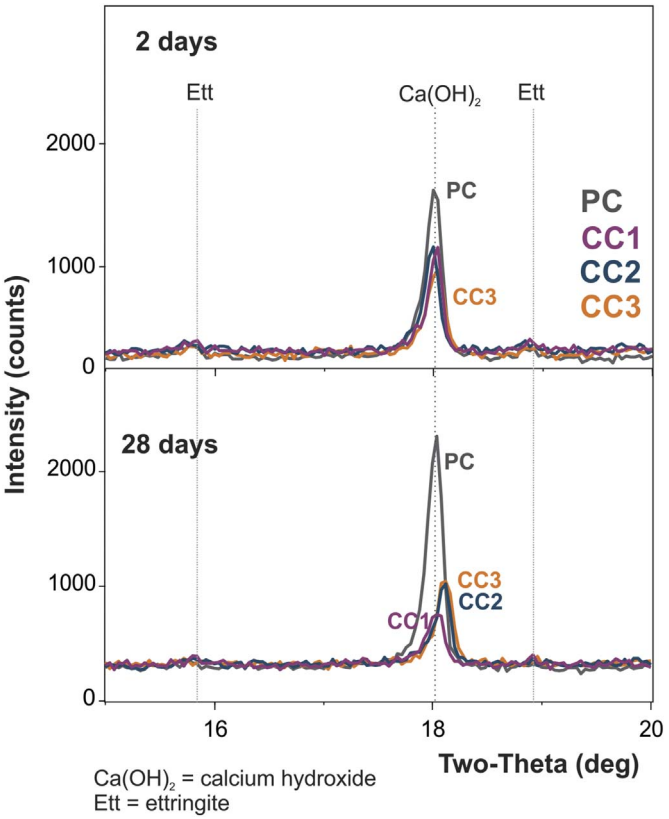

Fig. 13. XRD patterns for hydrated pastes at 2 days and 28 days.

25% calcined clay with 50 times minor surface area. The selection between increasing the degree of grinding, or increasing the percentage of replacement depends on an energy balance and quantity of available material.

Previous studies (Tironi et al., 2012a) determined that the high degree of structural disorder in kaolinite, before calcination, contributes largely to CS between 7 and 28 days. In this study was determined that the morphology of halloysite is an important characteristic. Yuan (2016) conclude that the tubular structure of halloysite overall demonstrates high thermal persistence, and the morphology and the porosity almost did not change until 900 °C or even at higher temperatures. The morphology of the studied clays does not modify drastically after thermal treatment, and the tubes and spheres were slightly affected by dehydroxylation process (Fig. 9). The spheroidal morphology of halloysite and platy kaolinite imparts the highest pozzolanic reactivity at early age (Fig. 11) and contributes to the CS (Fig. 12, Table 3); whereas tubular morphology has a good reactivity at early age, that increases extensively at later age contributing to the compressive strength at 28 days (Fig. 12, Table 3). The difference between two morphologies in pozzolanic activity is probably due to that the reactive surface is more accessible in spheroidal halloysite and platy kaolinite than in the tubular halloysite.

The tubular halloysite has the Al-OH sheet forming the inside and the Si—O sheet the outside (Pasbakhsh et al., 2013; Yuan et al., 2015). The pozzolanic reaction occurs first between $Ca(OH)_2$ released by PC-hydration and the Si—O sheet of the outside, and then between $Ca(OH)_2$ and reactive alumina inside of tubes. For platy kaolinite and spheroidal halloysite, the exposed surface contents reactive silica and reactive alumina, and the pozzolanic reaction occur with both. This difference in access and composition of the surface produces a faster pozzolanic reaction when the morphology is platy and spheroidal and the reactive alumina is easily available, however the later reactivity of the alumina in tubular halloysite produces different assemblage of the hydrated phases and a high contribution to compressive strength at later age.

5. Conclusions

Based on electrical conductivity test, Frattini test and compressive strength index, the three natural clays here studied with high content of halloysite/kaolinite, calcined at 700 °C and ground to 80% of particles with a size of < 45 μm, are classified as high reactive pozzolana.

The flowability of mortars elaborated with 25% of calcined halloysite/kaolinite clays as replacement of PC decreases significantly, and this effect was lower when the clay with 60/40 halloysite/kaolinite was used.

At different ages, the compressive strength depends on the halloysite/kaolinite ratio and the morphology of halloysite. The presence of kaolinite and spheroidal halloysite has a positive influence at early ages; tubular halloysite at later ages.

Since for spheroidal halloysite and kaolinite the reactive alumina is more easily available, the pozzolanic reaction occurs early. Whereas for tubular halloysite, the reaction of alumina is delayed producing different assemblages of hydrated phases and contributing to enhance the compressive strength at later ages.

References

Alujas, A., Fernández, R., Quintana, R., Scrivener, K.L., Martirena, F., 2015. Pozzolanic reactivity of low grade kaolinitic clays: influence of calcination temperature and impact of calcination products on OPC hydration. Appl. Clay Sci. 108, 94–101.

Bich, Ch., Ambroise, J., Péra, J., 2009. Influence of degree of dehydroxylation on the pozzolanic activity of metakaolin. Appl. Clay Sci. 44, 194–200.

Churchman, G.J., Whiton, J.S., Claridge, G.G.C., Theng, R.K.G., 1984. Intercalation method using formamide for differentiation halloysite from kaolinite. Clay Clay Miner. 32, 241–248.

Churchman, G.J., Pontifex, I.R., McClure, S.G., 2010. Factors influencing the formation and characteristics of halloysites or kaolinites in granitic and tuffaceous saprolites in Hong Kong. Clay Clay Miner. 58, 220–237.

Cravero, F., Fernández, L., Marfíl, S., Sánchez, M., Maiza, P., Martínez, A., 2016. Spheroidal halloysites from Patagonia, Argentina: some aspects of their formation and applications. Appl. Clay Sci. 131, 48–58.

Du, M., Guo, B., Jia, D., 2006. Thermal stability and flame retardant effects of halloysite nanotubes on poly(propylene). Eur. Polym. J. 42, 1362–1369.

Farzadnia, N., Ali, A.A.A., Demirboga, R., Anwar, M.P., 2013. Effect of halloysite nanoclay on mechanical properties, thermal behavior and microstructure of cement mortars. Cem. Concr. Res. 48, 97–104.

Fernandez, R., Martirena, F., Scrivener, K.L., 2011. The origin of the pozzolanic activity of calcined clay minerals: a comparison between kaolinite, illite and montmorillonite. Cem. Concr. Res. 41, 113–122.

Fernández, L.G., Cravero, F., Sánchez, M.P., De la Cruz Vivanco, C., Gatti, M., 2015. Synthesis and characterization of vinyltrimethoxysilane-grafted non-swelling clay. Procedia Mater. Sci. 8, 414–423.

Kakali, G., Perraki, T., Tsivilis, S., Badogiannis, E., 2001. Thermal treatment of kaolin: the effect of mineralogy on the pozzolanic activity. Appl. Clay Sci. 20, 73–80.

Luxan, M.P., Madruga, M., Saavedra, J., 1989. Rapid evaluation of pozzolanic activity of natural products by conductivity measurement. Cem. Concr. Res. 19, 63–68.

M'barek Jemaï, M.B., Sdiri, A., Errais, E., Duplay, J., Saleh, I.B., Zagrarni, M.F., Bouaziz, S., 2015. Characterization of the Ain Khemouda halloysite (western Tunisia) for ceramic industry. J. Afr. Earth Sci. 111, 194–201.

Morsy, M.S., Alsayed, S.H., Aqel, M., 2010. Effect of nano-clay on mechanical properties and microstructure of ordinary Portland cement mortar. Int. J. Civil Env. Eng. 10, 21–25.

Murat, M., 1983. Hydration reaction and hardening of calcined clays and relatedminerals. II. Influence of mineralogical properties of the raw-kaolinite on the reactivity of metakaolinite. Cem. Concr. Res. 13, 511–518.

Pasbakhsh, P., Churchman, G.J., Keelin, J.L., 2013. Characterisation of properties of various halloysites relevant to their use as nanotubes and microfibre fillers. Appl. Clay Sci. 74, 47–57.

Rabehi, B., Boumchedda, K., Ghernouti, Y., 2012. Study of calcined halloysite clay as pozzolanic material and its potential use in mortars. Int. J. Phys. Sci. 7, 5179–5192.

Russell, J.D., 1987. Infrared methods. In: Wilson, M.J. (Ed.), A Handbook of Determinative Methods in Clay Mineralogy. Chapman and Hall, New York, pp. 133–173 (Chapter 4).

Siddique, R., Klaus, J., 2009. Influence of metakaolin on the properties of mortar and concrete: a review. Appl. Clay Sci. 43, 392–400.

Smith, M.E., Neal, G., Trigg, M.B., Drennan, J., 1993. Structural characterization of the thermal transformation of halloysite by solid-state NMR. Appl. Magn. Reson. 4 (1–2), 157–170.

Taylor-Lange, S.C., Lamon, E.L., Riding, K.A., Juenger, M.C.G., 2015. Calcined kaolinite–bentonite clay blends as supplementary cementitious materials. Appl. Clay Sci. 108, 84–93.

Tironi, A., Trezza, M.A., Scian, A.N., Irassar, E.F., 2012a. Kaolinitic calcined clays: factors affecting its performance as pozzolans. Constr. Build. Mater. 28, 276–281.

Tironi, A., Trezza, M., Irassar, E., Scian, A., 2012b. Thermal activation of bentonites for their use as pozzolan. Revista de la Constr. 11, 44–53.

Tironi, A., Trezza, M.A., Scian, A.N., Irassar, E.F., 2013. Assessment of pozzolanic activity of different calcined clays. Cem. Concr. Compos. 37, 319–327.

Tironi, A., Trezza, M.A., Scian, A.N., Irassar, E.F., 2014a. Potential use of Argentine kaolinitic clays as pozzolanic material. Appl. Clay Sci. 101, 468–476.

Tironi, A., Trezza, M.A., Scian, A.N., Irassar, E.F., 2014b. Thermal analysis to assess pozzolanic activity of calcined kaolinitic clays. J. Therm. Anal. Calorim. 147, 547–556.

Yu, Q., Sawayama, K., Sugita, S., Shoya, M., Isojima, Y., 1999. The reaction between rice husk ash and $Ca(OH)_2$ solution and the nature of its product. Cem. Concr. Res. 29, 37–43.

Yuan, P., 2016. Thermal-treatment-induced deformations and modifications of halloysite. In: Yuan, P., Thill, A., Bergaya, F. (Eds.), Developments in Clay Science. Nanosized Tubular Clay Minerals Halloysite and Imogolite, vol. 7. Elsevier Ltd., Amsterdam, pp. 137–166 (Chapter 7).

Yuan, P., Tan, D., Annabi-Bergaya, F., Yan, W., Fan, M., Liu, D., He, H., 2012. Changes in structure, morphology, porosity, and surface activity of mesoporous halloysite nanotubes ander heating. Clay Clay Miner. 60, 561–573.

Yuan, P., Tan, D., Annabi-Bergaya, F., 2015. Properties and applications of halloysite nanotubes: recent research advances and future prospects. Appl. Clay Sci. 112–113, 75–93.